Switched Model Predictive Control for Improved Transient and Steady-State Performance

***Abstract*—This work presents a novel switched Model Predictive Control (MPC) formulation for power converters. During transients, the proposed method uses horizon-one non-linear Finite Control Set MPC to drive the system towards the desired reference. When the converter state is close to the reference, the controller switches to linear operation, using an approximate converter model and a PWM modulator. As an illustrative example, the proposed switched MPC is applied to a Flying Capacitor Converter. As evidenced by experimental results, the proposed control strategy provides quick disturbance compensation, whilst at the same time, giving excellent steady-state performance.**

***Index Terms*—Power Electronics, Model Predictive Control, Switching Controllers.**

I. Introduction

Various formulations of Model Predictive Control (MPC) have emerged as promising alternatives for the control of power converters. Common to all approaches is the, at times implicit, on-line minimization of a suitable cost function to determine the switching patterns. In the context of power converters, it is convenient to classify MPC methods into two major categories, depending on how switching is treated [1], [2]. If the converter uses a modulator, then the duty cycle (or modulation index), $d[k]$, can be considered as the control input of the system, $u[k]$. Thus, in this case, the input will belong to a bounded continuous set, i.e., $u[k] = d[k] \in \mathbb{U} = [0, 1]^m$, where m is the number of inputs. Therefore, if the converter can be modeled as a linear system, then the so-called *Explicit MPC* strategy can be used to obtain the optimal control input [3]. The advantage of using this MPC method comes from the fact that the optimization can be solved off-line. Moreover, since this MPC formulation relies upon a modulator in its implementation, it has the potential to give good steady-state performance. It often provides zero-average tracking error an also concentrates the spectra of electrical variables at specific frequencies. In addition, depending on the modulation strategy employed, the number of switch commutations can also be fixed a priori. The main drawback of using Explicit MPC is that it is limited to power converters that can be modeled as linear systems. Some suboptimal solutions have been proposed to govern nonlinear systems. Nevertheless, the optimization problem needs, in general, to be solved on-line, which normally requires a high computational burden, see, e.g., [4]–[6]

Some efforts have been made in order to obtain fast predictive controller with constant switching frequency. One of the first one is the, so-called, Predictive-Direct Power Control (P-DPC) [7], [8]. This method uses a power model of the system and a set of predefined inverter voltage vector sequences, based on a space vector pattern. Thus, the commutation instants within a sampling period are calculated to minimize the active and reactive power tracking error. Recently, the so-called Modulated MPC (M^{2}MPC) was proposed to govern two-level inverters [9]. Similarly to P-DPC, this method also consider a space vector pattern as an input sequence. However, in this case, the problem is formulated in terms of the $\alpha\beta$ currents. Then, optimal duty cycles are obtained by minimizing the current tracking error, yielding an optimal switching pattern. Even though both P-DPC and M^{2}MPC provide a constant switching frequency, they have been only applied to linear power converters. Moreover, the inputs constraints are not considered in the optimization problem. Therefore, if the commutation instants obtained are large that the sampling period, then a simple saturation is implemented, which results in a suboptimal solution. This is particular important during transients.

A second class of MPC algorithms for power electronics is the, so-called, Finite Control Set MPC (FCS-MPC) [10], [11] (also known as direct MPC [12], [13]). In this group, control algorithms directly consider the power switch positions, $S[k]$ as control inputs of the converter, without using a modulator. Since each power switch can adopt only two positions, namely 1 or 0 (ON or OFF), the input is restricted to belong to a finite set of switch combinations, i.e., $u[k] = S[k] \in \mathbb{U} = \{0, 1\}^m$. Thus, the cost function can be evaluated for all possible switching patterns. The optimal switching action is directly applied at the converter; no modulation stage is required. One of the most important advantages of FCS-MPC, when compared to linear controllers and Explicit MPC, is the fact that this predictive technique can deal with converter topologies exhibiting highly non-linear behavior: All that is needed is to evaluate a discrete-time model of the converter. Moreover, multiple targets can be encompassed with ease. This is achieved by formulating the cost function accordingly, e.g., targeting a reduction of the common mode voltage [14], or switching loses [15]. Of course, the overall performance of the system may be diminished as the number and variety of target increases. FCS-MPC in general provides a fast and controlled transient response to changes in the load and/or references. In particular, by including safety limits for the electrical variables as constraints in the optimization, this MPC technique can tackle unwanted over-currents, which using other cotrol methods may appear during transients; see e.g., [16], where a converter power limitation is imposed in the control of an AFE rectifier. For recent applications of this predictive control technique see [17]–[21]. The main drawback of FCS-MPC when compared to PWM-based strategies (such as classical linear control or Explicit MPC) is the performance obtained during steady state, see [22]: Often, steady state errors and wide-spread spectra are observed. Despite the fact that spectra can be manipulated to some extent [11], [23],

there is a limit to what can be achieved with such schemes. The main reason resides in the poor temporal resolution of FCS-MPC when compared to PWM implementations.

The present work describes a novel MPC formulation for power converters based on the preliminary work [24], which combines the advantages of both MPC classes described above, i.e., with and without a modulator. Realizing that both strategies have complementary qualities, the control algorithm switches between operating modes depending on whether the converter is in transient or in steady state. To be more specific, taking into account a full-nonlinear model of the converter, FCS-MPC is used to quickly steer the converter states towards a neighborhood of the desired references. In this neighborhood, power converters can generally be well approximated by linear models. Hence, linear MPC is used to asymptotically reach the references.[1] Due to the switching nature of the control scheme, achieved spectra inherit desirable properties of the modulator employed. To highlight the benefits of the proposed switched MPC strategy, a Flying Capacitor Converter (FCC) is chosen as an illustrative example. The FCC is a good example of a non-linear power converter which requires to control not only the output current, but also the internal floating capacitor voltages. Therefore, it is a challenging topology from a control point of view. As evidenced by experimental results, the proposed method gives excellent performance, both during transients and also in steady state. This work extends [24] by given a proper design criteria of the switching controller bounds based on the converter analysis, which avoids chattering between controllers. In addition, extensive experiments are included to validate the performance of the proposed control strategy.

II. Switched MPC Formulation

MPC or receding horizon control [25] is a control technique where the control input to be applied to the system is obtained by solving, at each sampling instant, an optimal control problem, which uses the current system state to forecast over a finite horizon future system behavior. This generates an optimal control sequence. The control action to be applied to the plant is the first element of this sequence. A key advantage of MPC is that system constraints (e.g., voltage and current limitations) and nonlinearities can be directly taken into account in the formulation [2].

A. Converter Model and Cost Function

The present work adopts a discrete time formulation with fixed sampling frequency and thus considers a discrete-time model of the converter, written in state space form as

$$x[k+1] = f(x[k], u[k]), \quad k \in \{0, 1, 2, \dots\}, \tag{1}$$

where $x[k]$ represents the system states, $u[k]$ stands for the control inputs, and f describes the converter dynamics. Following most of the literature in power electronics and drives,

[1]Our approach is somewhat related to ideas underlying *dual mode MPC*; see [25]. Such methods are based on the idea of defining a so-called *terminal region*, in which a local controller is used to finally drive the system to the desired reference.

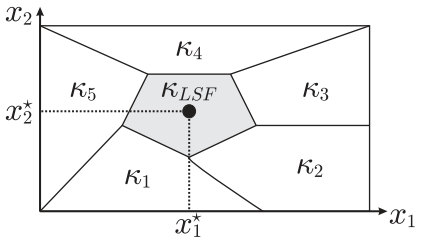

Figure 1. Illustration of the state space partition for Explicit MPC

a quadratic cost function with prediction horizon equal to one is used:

$$V(x[k], u) = \|x' - x^\star[k+1]\|_P^2, \tag{2}$$

where $x' = f(x[k], u)$, $\|v\|_P^2 \triangleq v^T P v$ denotes the weighted Euclidean norm, $x^\star$ refers to references, and

$$u \in \mathbb{U} \tag{3}$$

represents constraints on the decision variables, i.e., the gate signals. In (2), P is a positive semi-definite matrix, which contains the, so-called, weighting factors used to selectively penalize predicted components of the state, such as capacitor voltages, input or load currents, electrical torque, mechanical speed, etc.

On-line minimization of (2) subject to (3) at each discrete time step k yields the desired converter switching waveforms, represented by $u[k]$, $k \in \{0, 1, 2, \dots\}$. The resulting control law depends on the constraints imposed, as discussed next.

B. Basic Control Laws: FCS-MPC and Explicit MPC

In power converters, the switches operate either as an open-circuit or short-circuit. Thus, they can be described as binary variables. Therefore, by using $\mathbb{U} = \{0, 1\}^m$ in (3), where m is the number of complementary switches, one recovers FCS-MPC:

$$u[k] = \kappa_{FCS}(x[k]). \tag{4}$$

Given the converter state $x[k]$, $u[k]$ in (4) can be found through explicit enumeration, i.e., evaluating V in (2) for all 2^m permitted values of u to find, thus, the optimal input that minimizes the cost function, see also [13], [26], [27]. Here, it is important to emphasize that for FCS-MPC, f in (1), can be linear or nonlinear.

On the other hand, for power converters that can be (locally) modeled as a linear system by:

$$x[k+1] = Fx[k] + Gu[k], \tag{5}$$

and where the control input is synthesized through a PWM modulator, i.e., $\mathbb{U} = [0, 1]^m$ in (3), the minimization of (2) yields to linear MPC solutions. Here, it is possible to obtain a state space partition, which contains several polyhedral regions. Thus, an optimal explicit linear solution for each region is obtained, i.e.,

$$\kappa_i(x[k]) = K_i(x[k] - x^\star) + H_i. \tag{6}$$

Hence, the name Explicit MPC. The optimization procedure is carried out off-line. Afterwards, a lookup table containing K_i

and H_i is used to implement the optimal input to be applied. Consequently, the on-line algorithm is focused on determining which region the system-state belongs.

The number and size of these regions, as well as the values of K_i and H_i, depend on the systems constraints, system reference $x^\star$, and prediction horizon N. However, for the *terminal* region, which contains the reference, the optimal solution is always the same. This is the, so-called, unconstrained solution [28]. This can be optimally computed by solving $\partial V/\partial u = 0$, which yields the Linear State Feedback (LSF) control law:

$$u[k] = \kappa_{LSF}(x[k]), \tag{7}$$

with

$$\kappa_{LSF}(x[k]) = K(x[k] - x^\star[k]) + u^\star[k], \tag{8}$$

where, for the cost function (2),

$$K = -(G^T P G)^{-1} G^T P F,$$

and $u^\star[k]$ is the input required to maintain $x^\star[k]$, i.e.,

$$Gu^\star[k] = (I - F)x^\star[k].$$

This situation is illustrated in Fig. 1, where a state-space partition with 6 regions for a 2-state system is depicted.

To obtain a scheme which requires only a moderate computational effort, as described below, in the present approach MPC with a modulator is used only when the system state $x[k]$ is near its reference $x^\star[k]$. Thus, it is not necessary to obtain a system state partition and its associated local controllers. Therefore, only the explicit control law κ_{LSF} in (8) will be implemented. Here, it is important to highlight that this approach is limited to converters that can be (locally) modeled as linear systems, i.e., f in (1) follows the linear model presented in (5).

C. Mode Switching

The proposed model predictive controller switches between the two control laws (4) and (8) by first evaluating, at each sampling instant k, the expression

$$J[k] \triangleq \|x[k] - x^\star[k]\|_P^2, \tag{9}$$

cf., (2). If $J[k]$ is large, then the system is far from the desired terminal region. To achieve fast convergence to the neighborhood of $x^\star[k]$, the FCS-MPC law κ_{FCS} is used. If the system is in the terminal region, where the linear model of the system is valid, the controller utilizes κ_{LSF}, thereby, achieving a zero steady-state error. In fig. 2, a flow diagram of the proposed switched MPC strategy is shown. To avoid chattering, a hysteresis band with parameters J_L and J_H is introduced, see Fig. 3. The upper threshold J_H should be chosen small enough for the local model (5) to be accurate and also to allow timely detection of transient operation. Its size is limited by the necessity to avoid *false-triggering* due to noise and switching effects inherent to steady-state operation. Since FCS-MPC will drive the converter state only to a bounded region around the reference, the lower threshold J_L should be chosen large enough to allow the controller to switch back to steady state operation after a transient. Note that both

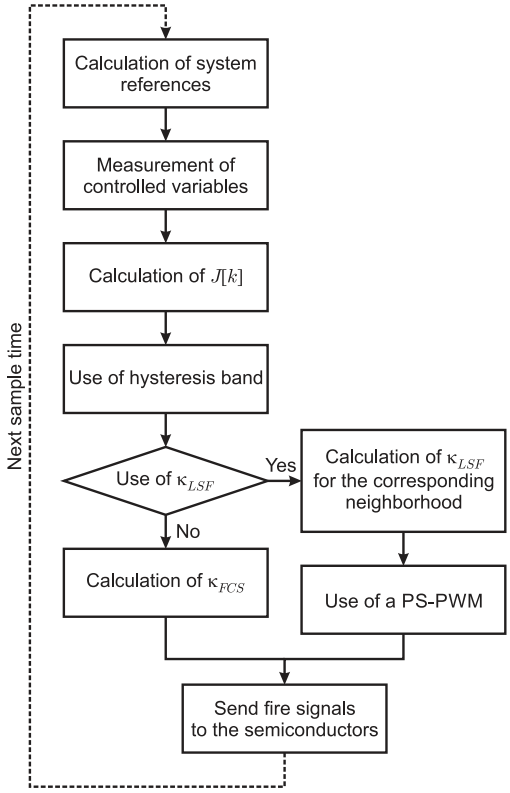

Figure 2. Flow diagram of the proposed Switched MPC strategy.

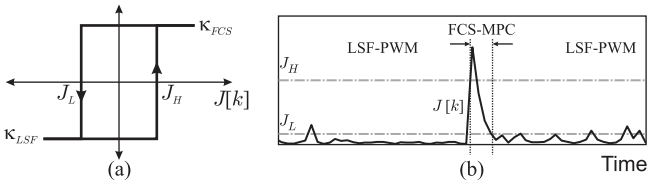

Figure 3. (a) Hysteresis band; (b) Controller switching triggered by $J[k]$.

controllers do not need to be initialized. Thus, only one active control strategy needs to be evaluated at each sampling instant. A specific design guideline is provided in Section IV.

III. Case Study: Flying Capacitor Converter

The proposed switched MPC algorithm can be applied to a variety of converter topologies, provided they can be locally described by a linear model of the form (5).

To highlight the advantages of the proposed control strategy, the present work considers an FCC as an illustrative example. This is an interesting topology for medium voltage applications [29]. Similar to the Neutral Point Converter topology [30], the FCC requires a single main dc-link for three-phase application. In this work, a three-cell FCC will be considered, as shown in Fig. 4. However, the analysis can be easily extended to any cell number.

By taking the system state and control input as

$$x[k] = \begin{bmatrix} v_{c1}[k] \\ v_{c2}[k] \\ i_a[k] \end{bmatrix}, \; u[k] = \begin{bmatrix} S_1[k] \\ S_2[k] \\ S_3[k] \end{bmatrix},$$

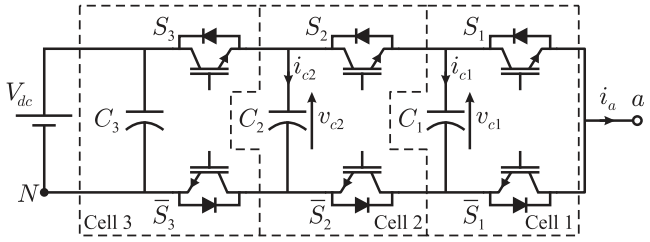

Figure 4. Three-cell (four-level) single-phase FCC.

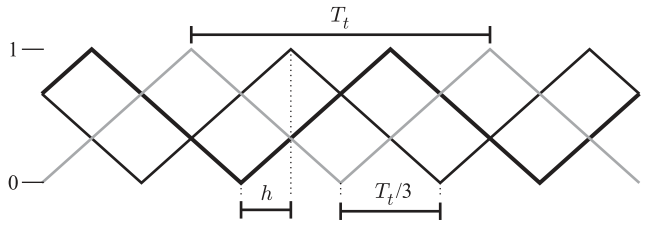

Figure 5. Triangular carriers used for the PWM modulator and the FCS-MPC

in [24] the following discrete-time model was obtained:

$$x[k+1] = Ax[k] + B(x[k])u[k], \tag{10}$$

where

$$B(x[k]) = \begin{bmatrix} -\frac{h}{C_1}x_3[k] & \frac{h}{C_1}x_3[k] & 0 \\ 0 & -\frac{h}{C_2}x_3[k] & \frac{h}{C_2}x_3[k] \\ k_b x_1[k] & k_b(x_2[k]-x_1[k]) & k_b(V_{dc}-x_2[k]) \end{bmatrix},$$

$$A = \begin{bmatrix} 1 & 0 & 0 \\ 0 & 1 & 0 \\ 0 & 0 & k_a \end{bmatrix},\ k_a = e^{-hR/L},\ k_b = (1-k_a)/R$$

and h denotes the sampling period.

In order to achieve the desired *balanced voltage condition* (11), a closed loop controller for an FCC should not only govern the output current, but also the internal floating voltages, where

$$v_{cy}^{\star} = \lambda \frac{V_{dc}}{n}, \qquad \lambda \in \{1, \ldots, n\}, \tag{11}$$

cf., [31], [32]. In this way, all semiconductors can be designed to block a voltage of V_{dc}/n. A multilevel output voltage waveform of $n+1$ levels can be, thus, obtained. Therefore, from a control viewpoint, an FCC is a challenging topology which presents nonlinearities described in $B(x[k])$.

When the system is far from the reference, the switched control strategy proposed in Section II-C applies FCS-MPC. To design this controller, matrix P in the cost function (2) is chosen as $P = \text{diag}\{\sigma_1, \sigma_2, \sigma_3\}$. Here, $\sigma_i > 0$ are design parameters (weighting factors), which allow one to trade current tracking errors for deviations in capacitor voltages. To obtain predictions of the system state when it is far from the reference, the nonlinear system (10) is directly evaluated for the 8 different combinations of $u[k]$, namely,

$$\mathbb{U} \triangleq \left\{ \begin{bmatrix}0\\0\\0\end{bmatrix}, \begin{bmatrix}0\\0\\1\end{bmatrix}, \begin{bmatrix}0\\1\\0\end{bmatrix}, \begin{bmatrix}0\\1\\1\end{bmatrix}, \begin{bmatrix}1\\0\\0\end{bmatrix}, \begin{bmatrix}1\\0\\1\end{bmatrix}, \begin{bmatrix}1\\1\\0\end{bmatrix}, \begin{bmatrix}1\\1\\1\end{bmatrix} \right\}. \tag{12}$$

The combination in $\mathbb{U}$ that minimizes (2) is applied during the entire sampling period h.

On the other hand, when the system state is close to the reference, the LSF control law (8) will be used in conjunction with Phase-Shifted PWM (PS-PWM). Thus, a natural balance of the floating voltages can be achieved [33] [2]. Since the modulator guarantees that the capacitor voltages remain balanced, one can consider them, in this case, as constant values. Thus, only the output current needs to be controlled. Therefore, the system is reduced to only one state, i.e., $x[k] = i_a[k]$, and the control input becomes $u[k] = d[k]$, yielding a linear first-order system:

$$x[k+1] = Fx[k] + Gu[k],$$

with $F = k_a$ and $G = k_b V_{dc}$, see (10). Consequently, the control law in (8) is designed using the above model and a reduced weighting matrix, namely, $P = \sigma_3$.

[2]Here, PS-PWM is preferred since it is easy to implement. However, any modulation strategy that guarantees the capacitor voltage balance can be used. See e.g. [34]–[36], where PD- and SV-PWM is considered.

Table I
MAIN CONVERTER AND CONTROLLER PARAMETERS.

Parameter	Value
V_{dc}	240 V
R	22 Ω
L	16.5 mH
C_1=C_2	330 μF
$\sigma_1 = \sigma_2$	0.1
σ_3	1
K	5
J_L	4
J_H	25
h	125 μs
T_t	750 μs

IV. EXPERIMENTAL RESULTS

The present section shows via experimental results that the switched model predictive controller proposed in Section II has the potential to outperform both linear control and FCS-MPC. The most relevant converter and control parameters are detailed in Table I. In this case, the weighting factors in P are chosen to achieve a fast dynamic, since FCS-MPC is only used to steer the system near the reference. When the LSF controller is used, the optimal voltage will be synthesized by using a modulator. Thus, the steady-state load current ripple and THD are imposed by the PS-PWM and the electrical load. The hysteresis band parameter J_L is designed based on simulations and using the criteria mentioned at the end of Section II-C. Motivated by the use of PWM, J_H is obtained considering zero steady-state error in the current tracking as follows: under this assumption $J[k]$ depends only on the floating voltages deviation, which can be upper bounded to their maximum values as per

$$\widehat{\Delta}_v = \frac{1}{C_x}\hat{\imath}\, T_t,$$

where C_x is the capacitance of the respective floating capacitor, $\hat{\imath}$ the maximum value of the output current, and T_t is the

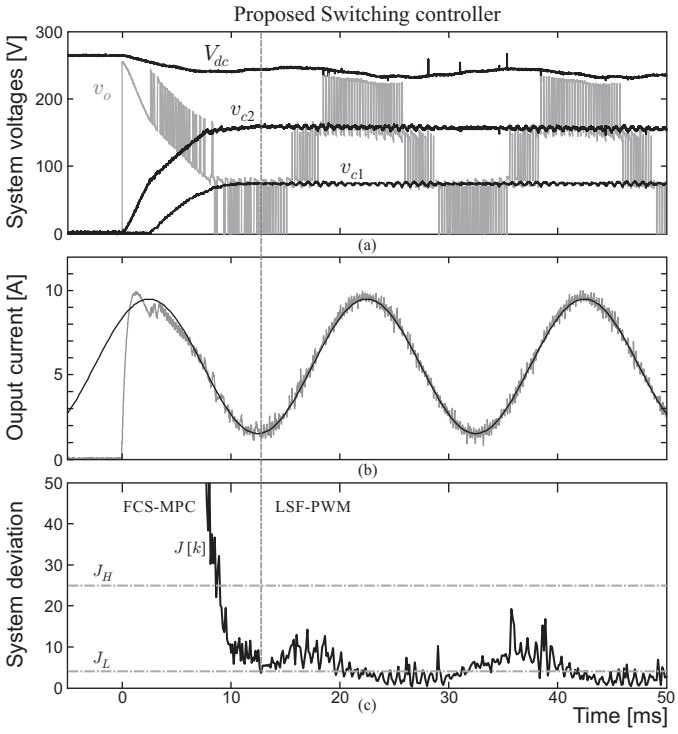

Figure 6. Start-up using the proposed switched MPC: (a) FCC inner and output voltages; (b) Output current; (c) System deviation $J[k]$; (d) FCC inner and output voltages

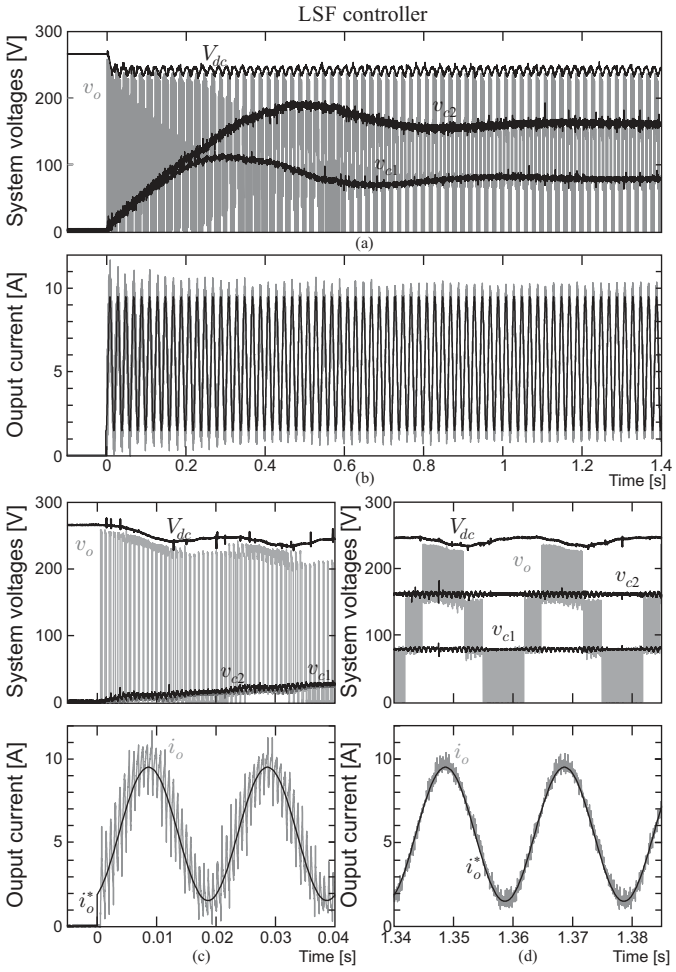

Figure 7. Start-up using an LSF controller: (a) FCC inner and output voltages; (b) Output current; (c) Relevant waveforms at the beginning of the start-up; (d) Relevant waveforms in steady-state.

carrier period, see Fig. 5. Then,

$$J_H > \left(\frac{\sigma_1}{C_1} + \frac{\sigma_2}{C_2}\right) \hat{\imath} T_t. \tag{13}$$

To avoid false triggering due to measurement noise, a larger value than in (13) should be used.

Three phase-shifted triangular carriers of 1333Hz (a frequency in the range of the industrial medium voltage converters [37] and previous published works [38]) are used for the PS-PWM required when the LSF controller (7) is used to govern the converter, obtaining an effective switching frequency of 4kHz at the converter output. These triangular carriers are also used to sample the converter states at the top and bottom of each carrier. Thus, a sampling period of $h = 125\mu$s is obtained, see Fig. 5.

The switched MPC algorithm of Section II is implemented in a digital control platform composed by a TMS320C6713 DSP and a XC3S400 FPGA Since only one controller is evaluated at each sampling instant, h, the execution time required for the proposed switched predictive control strategy is variable. It takes 14.2μs when FCS-MPC is evaluated and only 4.3μs when the LSF is implemented. The same sampling period, h, is used independently on which controller is evaluated.

A. Start-up Performance

One of the most demanding tests for a control scheme of an FCC is the start-up process without pre-charging the floating capacitors.[3] Fig. 6(a) and (b) show experimental voltages and output current obtained with the proposed switched MPC. At $t = 0$, the floating capacitor voltage errors are extremely high and the system deviation $J[k]$ exceeds the upper boundary J_H, thereby, activating the FCS-MPC mode. This can be appreciated in Fig. 6(c). Here, FCS-MPC rapidly leads the output current to its reference value. Thus, $J[k]$, during a start-up process, depends mostly on the floating capacitor voltage errors. Since FCS-MPC considers the complete nonlinear model of the converter (10) and an active control of v_{cx} through (2), the floating capacitor voltages are rapidly led to the desired balance values (11) in approximately 10ms. Once the output current and the floating voltages are near their references, $J[k]$ is reduced. When $J[k] \leq J_L$ the proposed scheme switches to the LSF controller mode, as the terminal region has been reached, see vertical dashed line in Fig. 6. It is important to remark that, in this operation mode, the floating voltages balance relies on the natural balance property guaranteed by the PS-PWM. For comparison, Fig. 7(a)-(d) illustrates the start-up process for the pure LSF controller.

[3]In practice, such a situation should be avoided due to the large blocking voltage in $S_3 - \overline{S}_3$ required.

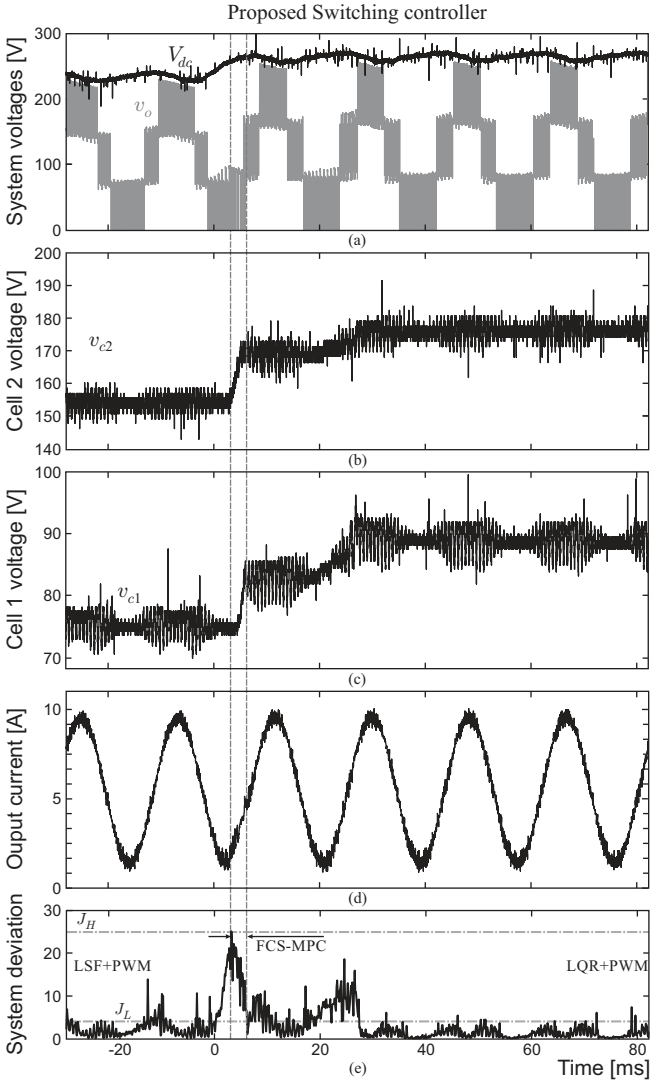

Figure 8. System behavior for a main dc-link disturbance using the proposed switched MPC formulation: (a) Main dc-link and output voltages; (b) v_{dc2}; (c) v_{dc1}; (d) Output current; (e) System deviation

In this case, the response is significantly slower than with the proposed controller. In particular, the floating voltages take about 1s to reach a steady-state. Moreover, with κ_{LSF} a significant overshoot in the voltages can be appreciated, which could significantly harm the floating capacitors. The effect of the floating voltages imbalance can also be appreciated in the output current, which has a large ripple at the beginning of the start-up, due to the essentially two-level output voltage v_o.

For both cases examined above, the output current reference used is given by:

$$i_a^\star = 5.5 + 4\,\sin(2\pi 50\,t),$$

Since the proposed scheme uses FCS-MPC during the entire transient, the response is identical to the one obtained with a normal FCS-MPC controller with similar parameters. However, the system response once the references is achieved will be completely different as shown below in Section IV-D.

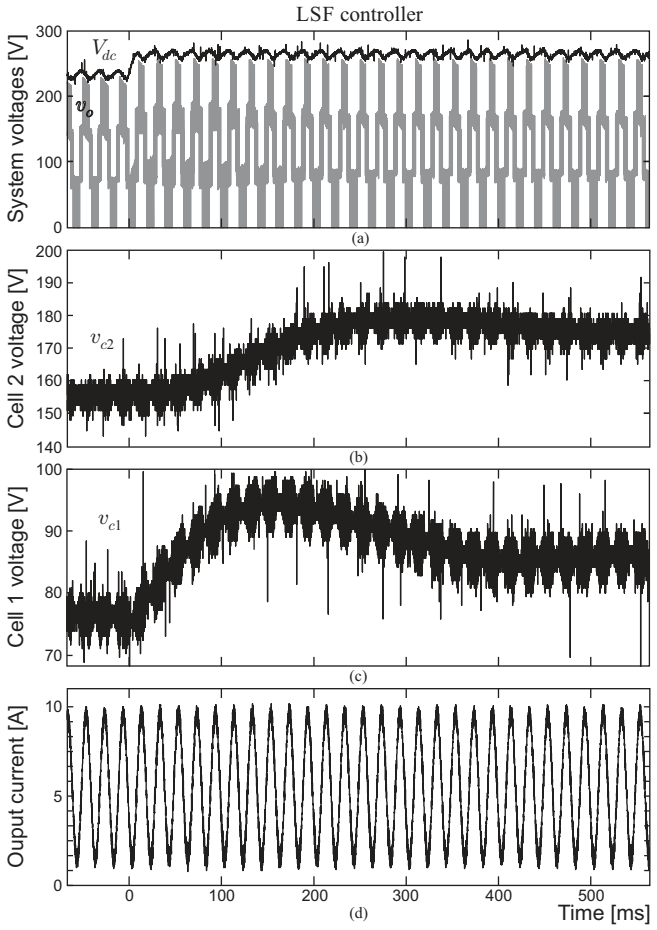

Figure 9. System behavior for a main dc-link disturbance using pure LSF controller: (a) Main dc-link and output voltages; (b) v_{dc2}; (h) v_{dc1}; (c) Output current

B. Main dc Voltage Disturbance

Figs. 8 and 9 illustrate the system behavior for a disturbance in the main dc-link voltage, which could have been caused by a network disturbance. Initially, the average main dc-link value is about 230V with corresponding floating voltages $v_{c1}^\star = 77$V and $v_{c2}^\star = 153$V. Since the current and voltages are near their reference values, $J[k]$ remains small and the proposed controller applies κ_{LSF}. At $t = 0$, the main dc-link voltage is rapidly increased to approx. 260V, yielding to new floating voltage references, i.e., $v_{c1}^\star = 87$V and $v_{c2}^\star = 173$V. This produced an increment of $J[k]$, which reaches J_H about 3ms after the main dc-link voltage starts to increase its value. This activates the FCS-MPC mode and the floating voltages are rapidly led to their new reference values, thereby, reducing $J[k]$. The use of FCS-MPC can also be appreciated in the output voltage (Fig. 8(a)) as a change in the pattern, and as a slightly change in the output current (Fig. 8(c)). At $t = 6$ms, $J[k]$ reaches J_L, and the system switches back to the LSF control law. Note that the floating voltages eventually reach their reference values through the natural balance property of the PS-PWM. Fig. 9(a)-(d) show the same maneuver when the system is controlled by a pure LSF controller. In this particular case, the transient takes about 500ms instead the 25ms achieved with the proposed switching

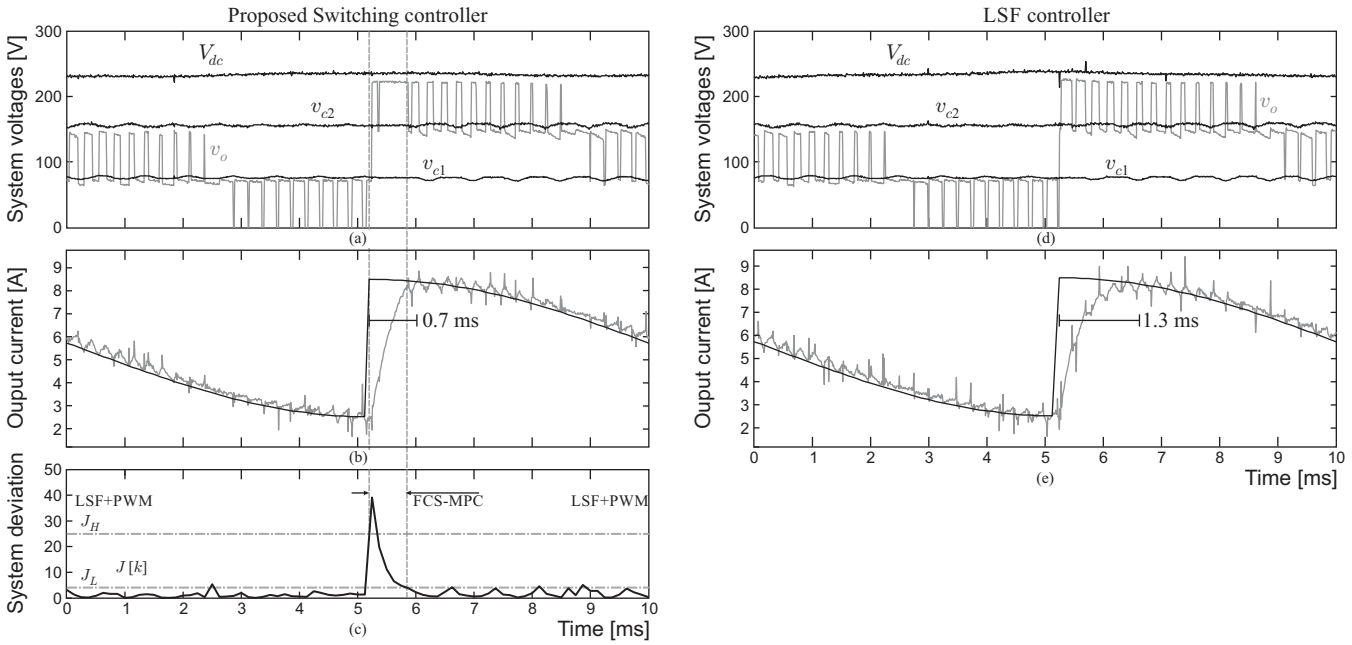

Figure 10. System response for a current reference step using the switched MPC formulation: (a) Inner and output voltages; (b) Output current; (c) System deviation; Using a pure LSF controller: (d) Inner and output voltages; (e) Output current.

controller. Moreover, and similarly to the start-up experiment discussed before, with pure LSF control, the floating voltages exhibit large oscillations.

C. Current Reference Tracking

In addition to significant gains obtained in start-up and disturbance compensation performance, the proposed controller of Section II also improves current tracking when compared to pure LSF controllers. This is illustrated in Fig. 10, where the reference is changed from $5.5 + 3\sin(2\pi 50t)$ to $5.5 - 3\sin(2\pi 50t)$ producing a 6A step change in the output current. Initially, $J[k]$ present a low value. Therefore, the switched MPC structure uses LSF, obtaining a typical PWM pattern. Once the reference change is applied, $J[k]$ increases, exceeding J_H, see Fig. 10(c). Thus, the controller switches to FCS-MPC operation. As can be appreciated in Fig. 10(a), a long pulse of magnitude V_{dc} in the output voltage, v_{aN}, is applied by FCS-MPC; therefore, the current increases at top speed and reaches the reference value in approximately 0.7ms. As the current approaches its reference, $J[k]$ decreases. Thus, the switched MPC goes back to the LSF control law. In contrast, Figs. 10(d) and (e) illustrate the response obtained when a pure LSF controller is employed. As can be seen, the response is almost two times slower than the response obtained with the proposed switching mode control scheme.

D. Steady-state Behaviour

The main advantage of the proposed control method when compared to linear state feedback controllers is its dynamic response, due to the judicious use of FCS-MPC. Once in steady-state, the switched MPC structure applies LSF. Therefore, well defined and concentrated spectra are obtained. Moreover, the commutation frequency of the switches is well known and is evenly distributed among them [24]. This is an important advantage of the proposed method, when compared to the results obtained with FCS-MPC, where the spectra are wide spread and the switches commutation frequency is uncertain. Figs. 11 and 12 shows the results obtained with an AC component of 1A and 4A over a 5.5A DC component respectively, confirming the previous statements. It is important to emphasize that the same sampling period, h, is used for both controller.

V. Conclusions

In this work a switched MPC formulation for power converters has been proposed. The control algorithm switches between non-linear Finite Control Set MPC without a modulator and linear state-feedback control with a modulator. The resulting switched model predictive controller exploits the advantages that both basic control methods offer: the fast transient response from FCS-MPC and accurate steady state operation provided by linear state-feedback controllers. The switching between these strategies is governed by how far the system variables are from their reference values, using a hysteresis band.

As an illustrative example, the proposed control method has been applied to a Flying Capacitor Converter prototype of 2.5kW feeding a passive load. Experiments showed that fast dynamic response can be obtained, even when the system non-linearities are more evident. In steady state, the output current tracks the reference, and power semiconductors operate at a constant switching frequency. Future work may include studying robustness to model imperfections and examining formulations with a larger prediction horizon.

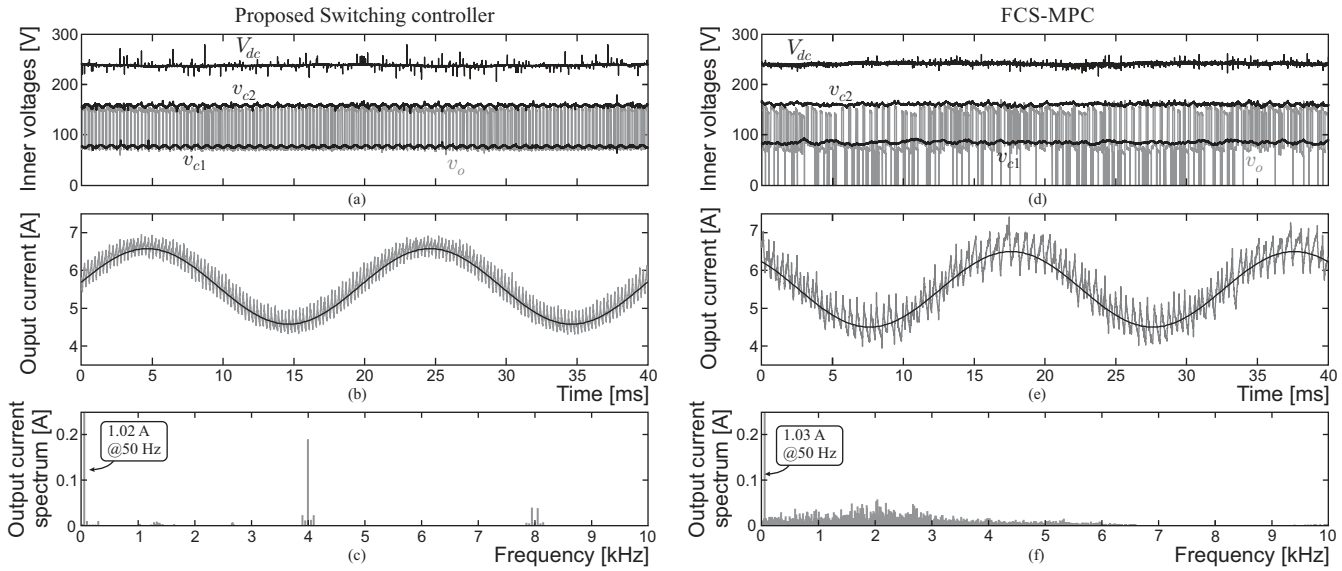

Figure 11. Steady-state response for a reference of $5.5 + \sin(2\pi 50t)$ using the proposed switched MPC structure: (a), (b), (c); Finite Control Set MPC: (d), (e), (f).

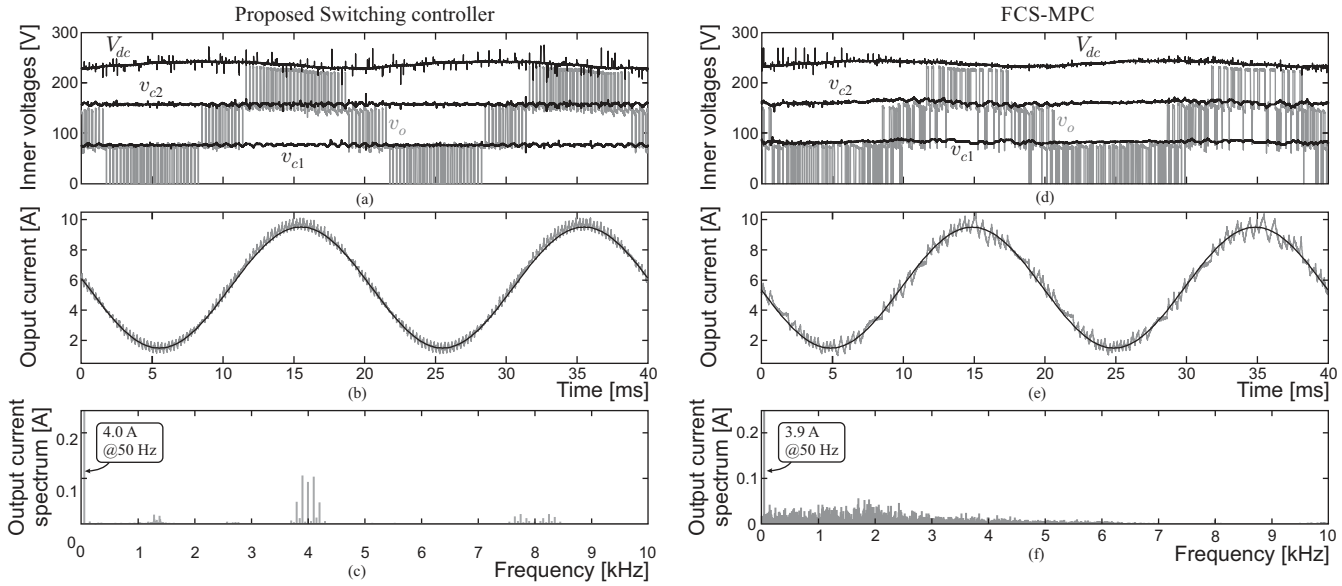

Figure 12. Steady-state response for a reference of $5.5 + 4\sin(2\pi 50t)$ with the proposed switched MPC structure: (a), (b), (c); using Finite Control Set MPC: (d), (e), (f).

REFERENCES

[1] P. Cortés, M. P. Kazmierkowski, R. M. Kennel, D. E. Quevedo, and J. Rodríguez, "Predictive Control in Power Electronics and Drives," *Industrial Electronics, IEEE Transactions on*, vol. 55, no. 12, pp. 4312–4324, Dec. 2008.

[2] D. E. Quevedo, R. P. Aguilera, and T. Geyer, "Predictive control in power electronics and drives: Basic concepts, theory, and methods," in *Advanced and Intelligent Control in Power Electronics and Drives*, ser. Studies in Computational Intelligence. Springer International Publishing, 2014, vol. 531, pp. 181–226.

[3] A. Linder and R. Kennel, "Model Predictive Control for Electrical Drives," in *Power Electronics Specialists Conference, 2005. PESC '05. IEEE 36th*, 2005, pp. 1793–1799.

[4] T. A. Johansen, I. Petersen, and O. Slupphaug, "Explicit sub-optimal linear quadratic regulation with state and input constraints," *Automatica*, vol. 38, pp. 1099–1111, 2002.

[5] N. Ameen, B. Galal, R. M. Kennel, and R. Kanchan, "The polynomial approximation of the explicit solution of model-based predictive controller for drive applications," *Predictive Control of Electrical Drives and Power Electronics (PRECEDE), 2011 Workshop on*, pp. 76–81, 2011.

[6] A. Grancharova, T. A. Johansen, and P. Tøndel, *Computational Aspects of Approximate Explicit Nonlinear Model Predictive Control*, ser. Lecture Notes in Control and Information Sciences, R. Findeisen, F. Allgöwer, and L. T. Biegler, Eds. Berlin, Heidelberg: Springer Berlin Heidelberg, 2007, vol. 358.

[7] S. Aurtenechea, M. A. Rodríguez, E. Oyarbide, and J. R. Torrealday, "Predictive Direct Power Control - A New Control Strategy for DC/AC Converters," in *IEEE Industrial Electronics, IECON 2006 - 32nd Annual Conference on*, 2006, pp. 1661–1666.

[8] S. Vazquez, A. Marquez, R. Aguilera, D. Quevedo, J. Leon, and L. Franquelo, "Predictive Optimal Switching Sequence Direct Power Control for Grid-Connected Power Converters," *IEEE Transactions on Industrial Electronics*, vol. 62, no. 4, pp. 2010–2020, 2015.

[9] L. Tarisciotti, P. Zanchetta, A. Watson, J. Clare, M. Degano, and S. Bifaretti, "Modulated Model Predictive Control for a Three-Phase Active Rectifier," *IEEE Transactions on Industry Applications*, vol. 51, no. 2, pp. 1610–1620, 2015.

[10] J. Rodríguez, M. P. Kazmierkowski, J. Espinoza, P. Zanchetta, H. Abu-Rub, H. A. Young, and C. A. Rojas, "State of the Art of Finite Control Set Model Predictive Control in Power Electronics," *IEEE Transactions on Industrial Informatics*, vol. 9, no. 2, pp. 1003–1016, May 2013.

[11] P. Cortés, J. Rodríguez, D. E. Quevedo, and C. Silva, "Predictive current control strategy with imposed load current spectrum," *IEEE Trans. Power Electron.*, vol. 23, no. 2, pp. 612–618, Mar. 2008.

[12] A. Linder and R. Kennel, "Direct model predictive control - a new direct predictive control strategy for electrical drives," in *Power Electronics and Applications, 2005 European Conference on*, 2005, p. 10.

[13] T. Geyer and D. E. Quevedo, "Multistep Finite Control Set Model Predictive Control for Power Electronics," *IEEE Transactions on Power Electronics*, vol. 29, no. 12, pp. 6836–6846, Dec. 2014.

[14] R. Vargas, U. Ammann, J. Rodríguez, and J. Pontt, "Predictive Strategy to Control Common-Mode Voltage in Loads Fed by Matrix Converters," *Industrial Electronics, IEEE Transactions on*, vol. 55, no. 12, pp. 4372–4380, 2008.

[15] R. Vargas, U. Ammann, and J. Rodríguez, "Predictive Approach to Increase Efficiency and Reduce Switching Losses on Matrix Converters," *Power Electronics, IEEE Transactions on*, vol. 24, no. 4, pp. 894–902, 2009.

[16] D. E. Quevedo, R. P. Aguilera, M. A. Pérez, P. Cortés, and R. Lizana, "Model Predictive Control of an AFE Rectifier With Dynamic References," *Power Electronics, IEEE Transactions on*, vol. 27, no. 7, pp. 3128–3136, 2012.

[17] T. J. Vyncke, S. Thielemans, and J. A. Melkebeek, "Finite-Set Model-Based Predictive Control for Flying-Capacitor Converters: Cost Function Design and Efficient FPGA Implementation," *IEEE Transactions on Industrial Informatics*, vol. 9, no. 2, pp. 1113–1121, 2013.

[18] R. Portillo, S. Vázquez, J. León, M. M. Prats, and L. Franquelo, "Model Based Adaptive Direct Power Control for Three-Level NPC Converters," *IEEE Transactions on Industrial Informatics*, vol. 9, no. 2, pp. 1148–1157, 2013.

[19] D. du Toit, H. d. T. Mouton, R. Kennel, and P. Stolze, "Predictive Control of Series Stacked Flying-Capacitor Active Rectifiers," *IEEE Transactions on Industrial Informatics*, vol. 9, no. 2, pp. 697–707, 2013.

[20] R. Ramírez, J. Espinoza, P. Melín, M. Reyes, E. Espinosa, C. Silva, and E. Maurelia, "Predictive controller for a three-phase/single-phase voltage source converter cell," *IEEE Transactions on Industrial Informatics*, vol. 10, no. 3, pp. 1878–1889, Aug 2014.

[21] Z. Ma, S. Saeidi, and R. Kennel, "FPGA Implementation of Model Predictive Control with Constant Switching Frequency for PMSM Drives," *IEEE Transactions on Industrial Informatics*, vol. PP, no. 99, pp. 1–1, 2014.

[22] R. P. Aguilera, P. Lezana, and D. E. Quevedo, "Finite-control-set model predictive control with improved steady-state performance," *IEEE Trans. Ind. Inf.*, vol. 9, no. 2, pp. 658–667, May 2013.

[23] D. E. Quevedo and G. C. Goodwin, "Multistep optimal analog-to-digital conversion," *IEEE Trans. Circuits Syst. I*, vol. 52, no. 4, pp. 503–515, Mar. 2005.

[24] R. P. Aguilera, P. Lezana, and D. E. Quevedo, "A switched model predictive control formulation for flying capacitor converters," in *Proc. 15th International Power Electronics and Motion Control Conf., EPE-PEMC 2012 ECCE Europe*, Novi Sad, Serbia, 2012.

[25] J. Rawlings and D. Mayne, *Model Predictive Control: Theory and Design*. Nob Hill Publishing, 2009.

[26] D. E. Quevedo, G. C. Goodwin, and J. A. De Doná, "Finite constraint set receding horizon quadratic control," *Int. J. Robust Nonlin. Contr.*, vol. 14, no. 4, pp. 355–377, Mar. 2004.

[27] R. P. Aguilera and D. E. Quevedo, "Stability Analysis of Quadratic MPC with a Discrete Input Alphabet," *IEEE Transactions on Automatic Control*, vol. 58, no. 12, pp. 3190–3196, Dec. 2013.

[28] J. A. De Doná, G. C. Goodwin, and M. M. Serón, *Constrained Control & Estimation – An Optimization Perspective*. London: Springer-Verlag, 2005.

[29] T. Meynard, M. Fadel, and N. Aouda, "Modeling of multilevel converters," *Industrial Electronics, IEEE Transactions on*, vol. 44, no. 3, pp. 356–364, 1997.

[30] A. Nabae, I. Takahashi, and H. Akagi, "A New Neutral-Point-Clamped PWM Inverter," *Industry Applications, IEEE Transactions on*, no. 5, pp. 518–523, 1981.

[31] P. Lezana, R. P. Aguilera, and D. E. Quevedo, "Model predictive control of an asymmetric flying capacitor converter," *IEEE Trans. Ind. Electron.*, vol. 56, no. 6, pp. 1839–1846, Jun. 2009.

[32] E. Silva, B. McGrath, D. E. Quevedo, and G. Goodwin, "Predictive Control of a Flying Capacitor Converter," in *American Control Conference, 2007. ACC '07*, 2007, pp. 3763–3768.

[33] R. Wilkinson, T. Meynard, and H. du Toit Mouton, "Natural Balance of Multicell Converters: The General Case," *Power Electronics, IEEE Transactions on*, vol. 21, no. 6, pp. 1658–1666, 2006.

[34] B. McGrath and D. Holmes, "Enhanced Voltage Balancing of a Flying Capacitor Multilevel Converter Using Phase Disposition (PD) Modulation," *IEEE Transactions on Power Electronics*, vol. 26, no. 7, pp. 1933–1942, 2011.

[35] A. Shukla, A. Ghosh, and A. Joshi, "Natural Balancing of Flying Capacitor Voltages in Multicell Inverter Under PD Carrier-Based PWM," *IEEE Transactions on Power Electronics*, vol. 26, no. 6, pp. 1682–1693, 2011.

[36] S. Choi and M. Saeedifard, "Capacitor Voltage Balancing of Flying Capacitor Multilevel Converters by Space Vector PWM," *IEEE Transactions on Power Delivery*, vol. 27, no. 3, pp. 1154–1161, 2012.

[37] T. Meynard, H. Foch, P. Thomas, J. Courault, R. Jakob, and M. Nahrstaedt, "Multicell converters: basic concepts and industry applications," *IEEE Transactions on Industrial Electronics*, vol. 49, no. 5, pp. 955–964, Oct 2002.

[38] S. Fazel, S. Bernet, D. Krug, and K. Jalili, "Design and comparison of 4-kv neutral-point-clamped, flying-capacitor, and series-connected h-bridge multilevel converters," *Industry Applications, IEEE Transactions on*, vol. 43, no. 4, pp. 1032–1040, July 2007.